Renormalization for the boundary of chaos in piecewise monotonic maps with a single discontinuity

Paul Glendinning

School of Mathematics
University of Manchester, Manchester M13 9PL, U.K.

E-mail: p.a.glendinning@manchester.ac.uk

Abstract. Monotonic maps with a single discontinuity arise in a variety of situations. We describe the infinite sets of periods for such maps on the boundary of chaos; this gives a sense of the routes to chaos in such maps. The description involves an explicit subshift of finite type which describes the sequences of different renormalizations possible in these maps.

PACS numbers: 05.45.-a

Keywords: renormalization, piecewise monotonic map, homoclinic bifurcation, hybrid system

Submitted to: *Nonlinearity*

1. Lorenz, isopleths and piecewise smooth maps

One-dimensional piecewise monotonic maps with a single discontinuity arise naturally in many situations. Early work was mostly associated with the study of global bifurcations, and in this case the maps have slopes which (typically) tend to zero or infinity as the point of discontinuity is approached from above or below [14, 15, 16, 17, 24]. On the other hand, linear maps are good models in a range of applications involving switching, so they have been studied within the literature of hybrid systems [6, 7, 8, 9]. A number of recent works have looked at these linear models in more detail [3, 4, 5]. This paper is concerned with routes to chaos in these maps, and in particular the sets of periods of orbits that can co-exist if the map is not chaotic. For the standard unimodal map the answer is very simple: the only periodic orbits that can exist in such maps which do not have positive topological entropy have period 2^n, and on the boundary of chaos, where a small perturbation can lead to positive topological entropy, the map has orbits of period 2^n for all $n \geq 0$. Here we identify implicitly all the infinite sets of periods

that can coexist on the boundary of chaos for piecewise monotonic maps with a single discontinuiity.

These maps were originally introduced in the applied literature through the study of generalizations of the Lorenz equations [23]:

$$\dot{x} = \sigma(y - x), \quad \dot{y} = rx - y - xz, \quad \dot{z} = xy - bz \tag{1}$$

where the parameter values considered by Lorenz were $\sigma = 10$, $r = 28$, and $b = 8/3$. There are many surprisingly modern touches in Lorenz's seminal 1963 paper [23]. Despite the somewhat dated computer simulations, which meant that Lorenz was only able to generate a few trajectories, these simulations were analyzed with remarkable sophistication. Of particular relevance to the problem addressed here are Figures 3 and 4 of [23]. In his Figure 4 Lorenz plots successive relative maxima of the z-coordinate against each other. This reveals an almost one-dimensional map $z_{n+1} = M(z_n)$ where the function M is continuous and has a cusp-like maximum about which the map appears symmetric. Figure 3 is more original; indeed I am not aware of an analogous analysis being undertaken subsequently in the dynamical systems literature although this may be because modern visualization techniques make it unnecessary. The idea of an *isopleth* is common in metereological studies: these are contours on which some quantity is constant, so isobars (constant pressure) and isotherms (constant temperature) are familiar examples. Lorenz plots isopleths of x in the (y, z)-plane for a numericaly computed trajectory. The results (his Figure 3) are striking. The isopleths are single valued over much of the projection of the attractor, and fold back across each other in regions where the isopleths can take two values. Thus, as Lorenz puts it, 'the trajectory is confined to a pair of surfaces which appear to merge in the lower portion of Fig. 3.' [23] The isopleth technique is effectively a way of visualizing the topology of the attractor.

In the mid-1970s, when mathematicians began to recognised the importance of Lorenz's analysis to the growing interest in chaotic behaviour, these two approaches were formalized in two different ways. Kaplan and Yorke [22], see also Sparrow [26] and Afraimovich et al [1, 2], took the idea of the succcessive maxima map and identified a related *discontinuous* map as arising naturally close to homoclinic bifurcations. Guckenheimer and Williams [28, 28] abstracted the isopleth surface to the classic Lorenz (branched) manifold. The curve on which the manifolds are glued together is a natural return section on which an abstract return map is defined, and because of the role of the stationary point at the origin, this return map has a discontinuity. At the discontinuity the form of the map depends on the linearized flow near the origin, which has three real eigenvalues. The ratio of the modulus of the leading stable and unstable eigenvalues determines the behaviour of the map at the discontinuity. If the unstable eigenvalue is stronger, as in the Lorenz equations, then the slope tends to infinity whilst if the stable eigenvalue is stronger then the slope tends to zero.

A further complication can be introduced if the branches of the Lorenz manifold are given a half-twist. These make the relevant branches of the return map decreasing rather than increasing. Thus there are four classes of maps with a single discontinuity

as illustrated in Figure 1: one with both branches increasing, one with both branches decreasing, and two with one increasing and one decreasing branch (these latter are related by reflection symmetry). In the following we are interested in these maps in the case that there is some contraction, so the results are particularly relevant to the case where the ratio of the stable and unstable eignevalues is less than one in modulus.

One of the most important steps towards understanding the possible routes to chaos involves determining the structure of maps on the boundary of chaos (in the sense of positive topological entropy). For unimodal (one-hump) maps such as the logistic map ($x \to \mu x(1-x)$) this is achieved by an inductive argument based on induced maps: either the map has a fixed point on its decreasing branch or it doesn't. In the latter case it is easy to show that the only attractors are fixed points and the dynamics is simple. In the former case one considers the second iterate of the map. If this does not map a pair of intervals (permuted by the original map) into themselves then there is positive entropy, and otherwise the second iterate restricted to either interval is again a unimodal map and we can ask the same question again. If the induced map has a fixed point on its decreasing branch then this must be an orbit of period 2 for the original map and the argument repeats, looking at the second iterate of the second iterate, i.e. f^4. For maps on the boundary of chaos (in the smooth setting) the induced maps of the induced maps can always be defined, these are called *infinitely renormalizable*, and hence have orbits of period 2^n for $n = 0, 1, 2, \ldots$. Whilst there are other possible renormalizations for one-hump maps at appropriate parameter values, the second iterate (and the second iterate of the second iterate etc) are the only ones that leave behind a zero entropy set, so they are the only ones relevant to the boundary of chaos.

One of the aims of this paper is to generalize this argument to the maps shown in Figure 1. We do this by concentrating on maps on the boundary of chaos which are infinitely renormalizable, characterizing these maps by the set of periods which exist for each map. More precisely, let $f : I \to I$ be a map of the interval I, then the set of (minimal) periods of f, $P(f)$, is defined to be

$$P(f) = \{n \in \mathbb{N} \mid f^n(x) = x \text{ some } x \in I, \text{ and } f^i(x) \neq x,\ 1 \leq i < n\} \quad (2)$$

Thus $P(f)$ is a (finite or infinite) set of positive integers. In the sense that families of maps which pass through a given map f on the boundary of chaos must create orbits with periods in $P(f)$ before becoming chaotic, this characterization gives some insight into the bifurcations which must occur in transitions to chaos via the map f. If a map is on the boundary of chaos and is not infinitely renormalizable it will still be renormalizable a finite number of times (possibly zero) and in this sense this paper gives a complete description of the possible periods on the boundary of chaos.

The maps in Figure 1 have three properties in common, there is a discontinuity at $x = 0$, they are continuous and monotonic in $x < 0$ and in $x > 0$, and there are continuously differentiable ($x \neq 0$) with slope tending to zero as x tends to zero from either above or below. Although this latter property is not fundamental here it is natural in the context of global bifurcation theory [17]. The boundary of chaos in

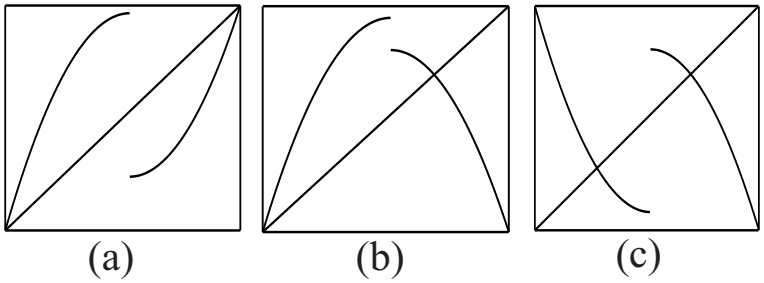

Figure 1. Monotonic maps with a single discontinuity: (a) Class A (orientable); (b) Class B (semi-orientable); and (c) Class C (non-orientable). Maps in class D are obtained from maps in class B by the transformation $x \to -x$. In each case the interval is $[z_0, z_1]$, with the definitions given in the text.

the case that both branches of the map are increasing (called Class A [17], Fig. 1(a)) has been described by Tresser [27]. Essentially the boundary of chaos (in a natural parameter space) consists of points on which maps have an infinite set of periods (p_n) related by $p_{n+1} = a_n p_n$, $a_n > 1$, and line segments on which maps have a finite set of periods (also satisfying $p_{n+1} = a_n p_n$). Since there are a number of papers on these cases, no further details will be given here [13, 24, 27].

The remaining three classes of maps are class B (increasing in $x < 0$, decreasing in $x > 0$), class C (decreasing in both $x < 0$ and $x > 0$) and class D (decreasing in $x < 0$ and increasing in $x > 0$). As noted earlier, maps in class B and class D are equivalent under the transformation $x \to -x$. For all these cases there are regions (in a suitably chosen parameter space) where maps on the boundary of chaos have the infinite set of periods (p_n) with

$$p_{n+1} = 2p_n + (-1)^n \tag{3}$$

This corresponds to transitions to chaos via the anharmonic route described in [15, 16]. This anharmonic route is described by a sequence of induced maps, or renormalizations, that oscillates between two classes. It is remarkable (for an appropriate class of maps) in that it is robust: a sufficiently small perturbation of a family that has this cascade of bifurcations to chaos has the same bifurcation structure (cf. period-doubling). By making explicit some remarks in [10, 17] it is possible to set up a subshift of finite type which describes how the boundary of chaos is mapped to itself under a number of renormalization operations which are the equivalents of the zero entropy renormalization of the unimodal map by f^2. The derivation of this subshift is the main result here: it enables us to give (implicitly) a description of all the possible infinite sets of periods for maps on the boundary of chaos in classes B, C and D. Note that these new infinitely renormalizable cases seem unlikely to have the robustness property of the anharmonic route

The methods used here echo the standard arguments rehearsed above for unimodal maps, and the underlying mathematical techniques will be familiar to those who know the kneading theory of Milnor and Thurston [25]. It is worth noting one caveat (to

which we return in the conclusion) before describing the detail. The analysis here is based on the assumption that the effect of the induced maps on the kneading invariants is a bijection in relevant parts of the space of possible kneading invariants. As such our analysis is akin to that of [13] for the orientable Class A. The symbolic arguments that would provide rigorous support for this assumption are long and have multiple sub-cases, see the appendix of [19] for an example of what would be involved, although recent arguments of [18] provide a short-cut here.

The remainder of the paper is organized as follows. In the next section we give formal definitions of the maps under consideration and the associated kneading theory is recalled in section 3. In section 4 the simple cases are analyzed (the equivalents of the simple case for unimodal maps when there is no fixed point on the branch with negative slope). Section 5 contains the main decomposition of parameter space and section 6 describes the subshift of finite type induced by the renormalization scheme. Some consequences of this are sketched in section 7 with examples of how the subshift can be used to generate sets of periods, whilst in the last two sections we return to the issue of the level of rigour (or lack of it) provided by the arguments presented.

2. Some definitions: maps and parameter space

We begin with the basic definition of the four classes of maps being considered and then go on to describe the parametrization of families of maps in each class. In all cases the interval the interval $I = [z_0, z_1]$ with $z_0 < c < z_1$ and the point of discontinuity of the map is at $x = c$.

Definition 2.1: A map $f : [z_0, z_1] \to [z_0, z_1]$ is monotonic with a single discontinuity (msdc) if
(i) f is continuous on $[z_0, z_1]\backslash\{c\}$;
(ii) $f|_{(z_0,c)}$ and $f|_{(c,z_1)}$ is strictly monotonic; and
(iii) $f(z_i) \in \{z_0, z_1\}$, $i = 0, 1$.

Note that the third condition is easy to relax, but we retain it as the boundary points will be important in the renormalization process. The four different classes of maps are obtained by choosing the branches of f to be increasing or decreasing in different combinations, together with simple conditions at the end-points of the interval. We use the notation $f(c_-) = \lim_{x\uparrow c} f(x)$ and $f(c_+) = \lim_{x\downarrow c} f(x)$.

Definition 2.2: A map $f : [z_0, z_1] \to [z_0, z_1]$ is in class A if it is msdc and
(i) $f|_{(z_0,c)}$ and $f|_{(c,z_1)}$ are strictly increasing; and
(ii) $f(z_0) = z_0$ and $f(z_1) = z_1$.

As noted in the introduction, the boundary of chaos of maps in class A is described in [13, 27].

Definition 2.3: A map $f : [z_0, z_1] \to [z_0, z_1]$ is in class B if it is msdc and
(i) $f|_{(z_0,c)}$ is strictly increasing and $f|_{(c,z_1)}$ is strictly decreasing; and
(ii) $f(z_0) = f(z_1) = z_0$.

Definition 2.4: A map $f : [z_0, z_1] \to [z_0, z_1]$ is in class C if it is msdc and
(i) $f|_{(z_0,c)}$ and $f|_{(c,z_1)}$ are strictly decreasing;
(ii) $f(z_i) = f(z_{1-i}), = 0, 1$.

Definition 2.5: A map $f : [z_0, z_1] \to [z_0, z_1]$ is in class D if it the map $g : [-z_1, -z_0] \to [-z_1, -z_0]$ defined by $g(x) = -f(-x)$, is in class B.

Maps in these four classes are determined (up to a semi-conjugacy which collapses only sinks and their preimages and wandering intervals to points) by two topological invariants: the kneading sequences of c_+ and c_- [10]. Hence it seems natural to work in a two-parameter space. All the results below are conjectured to be true in the space of kneading invariants, but to make matters more approachable we assume that there exist full two-parameter families of maps in each class so that the parameter space can be taken to be a connected closed subset of $\mathbb{R}^2$, cf. [17]. For example, the maps

$$A_{\mu,\nu}(x) = \begin{cases} \nu - x^2 & \text{if } x < 0 \\ -\mu + x^2 & \text{if } x > 0 \end{cases} \tag{4}$$

is in class A with $c = 0$ provided $(\mu, \nu) \in D_A$ defined by

$$D_A = \{(\mu, \nu) \mid -\frac{1}{4} \le \nu \le \mu(\mu + 1) \text{ and } -\frac{1}{4} \le \mu \le \nu(\nu + 1)\} \tag{5}$$

see Figure2a. We shall refer to the region D_A as an A-box. Ideally we would work with two-parameter full families of maps, i.e. families which realise every possible kneading invariant of the class, and more generally, an A-box for a full family of maps in class A parameterised by μ and ν, is a region bounded by the curves U_1 to U_4 defined by

$$\begin{aligned} U_1 &= \{\mathbf{a} \in \mathbb{R}^2 \mid f'_{\mathbf{a}}(z_0) = 1\} \\ U_2 &= \{\mathbf{a} \in \mathbb{R}^2 \mid f'_{\mathbf{a}}(z_1) = 1\} \\ U_3 &= \{\mathbf{a} \in \mathbb{R}^2 \mid f_{\mathbf{a}}(c^-) = z_1\} \\ U_4 &= \{\mathbf{a} \in \mathbb{R}^2 \mid f_{\mathbf{a}}(c^+) = z_0\} \end{aligned} \tag{6}$$

for which every kneading invariant is realised for at least one choice of $\mathbf{a}$. Note that the first two are the loci of saddlenode bifurcations creating the boundary fixed points, and the second to are homoclinic bifurcation points beyond which the interval $[z_0, z_1]$ is no longer invariant. For simplicity, we assume that these conditions do indeed define segments of continuous curves in the plane and that they bound a closed, connected set, D_A. Note that the quadratic family $A_{\mu,\nu}$ is not full [10, 11, 14].

Similar definitions can be given in the cases of full families of maps in class B (and hence class D) and class C (see Figure 2b,c). For a full family of maps, $(f_{\mathbf{a}})$ in class B, with $\mathbf{a} \in \mathbb{R}^2$, define

$$\begin{aligned} V_1 &= \{\mathbf{a} \in \mathbb{R}^2 \mid f'_{\mathbf{a}}(z_0) = 1\} \\ V_2 &= \{\mathbf{a} \in \mathbb{R}^2 \mid f_{\mathbf{a}}(c^-) = z_1\} \\ V_3 &= \{\mathbf{a} \in \mathbb{R}^2 \mid f_{\mathbf{a}}(c^+) = z_0\} \end{aligned} \tag{7}$$

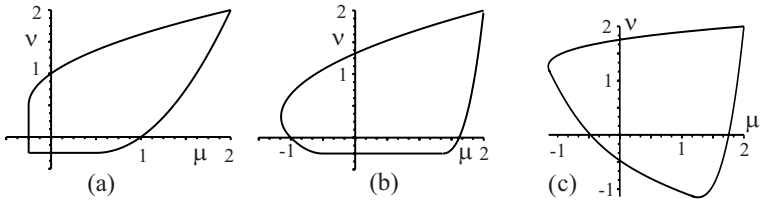

Figure 2. Parameter boxes in the (μ, ν)-plane for (a) Class A (orientable); (b) Class B (semi-orientable); and (c) Class C (non-orientable).

Then a B-box is the region bounded by these three curves. Note that both $V_1 \cap V_2$ and $V_1 \cap V_3$ correspond to degenerate cases of the maps for which we allow $z_1 = c$. In terms of the simple quadratic family

$$B_{\mu,\nu}(x) = \begin{cases} \nu - x^2 & \text{if } x < 0 \\ \mu - x^2 & \text{if } x > 0 \end{cases} \tag{8}$$

these curves are given by

$$\begin{aligned} V_1 &= \{(\mu, \nu) \mid \nu = -\tfrac{1}{4}\} \\ V_2 &= \{(\mu, \nu) \mid \nu = (\mu - \nu^2) + (\mu - \nu^2)^2\} \\ V_3 &= \{(\mu, \nu) \mid \nu = (\mu - \mu^2) + (\mu - \mu^2)^2\} \end{aligned} \tag{9}$$

Finally, for full families $(g_{\mathbf{a}})$ in class C, with a $\mathbf{a} \in \mathbb{R}^2$, define

$$\begin{aligned} W_1 &= \{\mathbf{a} \in \mathbb{R}^2 \mid (g_{\mathbf{a}}^2)'(z_i) = 1\} \\ W_2 &= \{\mathbf{a} \in \mathbb{R}^2 \mid g_{\mathbf{a}}(c^+) = z_1\} \\ W_3 &= \{\mathbf{a} \in \mathbb{R}^2 \mid g_{\mathbf{a}}(c^-) = z_0\} \end{aligned} \tag{10}$$

Then these three curves enclose the region D_C. As with case B, the intersections of these curves correspond to degenerate cases. Again, these curves are easy to calculate for the quadratic family

$$C_{\mu,\nu}(x) = \begin{cases} -\nu + x^2 & \text{if } x < 0 \\ \mu - x^2 & \text{if } x > 0 \end{cases} \tag{11}$$

W_1 does not have a simple close form (though it can be given explicitly using solutions of cubic equations), and is shown numerically in Figure 2c, and

$$\begin{aligned} W_2 &= \{(\mu, \nu) \mid \mu + \nu = (\mu - \mu^2)^2\} \\ W_3 &= \{(\mu, \nu) \mid \mu + \nu = (\nu - \nu^2)^2\} \end{aligned} \tag{12}$$

3. Kneading Theory

Kneading theory provides a symbolic description of iterates of maps. Maps can be identified (up to sets of periodic orbits with the same code and homtervals, i.e. intervals on which f^n is monotonic for all n; these intervals can include parts of the local basins of attraction of stable periodic orbits if they exist) by their kneading invariant: a pair of sequences associated with orbits obtained by approaching the critical point c from

above or below. The material presented here is standard, although the different cases are not usually described together.

Let $f : I \to I$ be a msdc map with discontinuity $c \in I$, and define

$$a(x) = \begin{cases} -1 & \text{if } x < c \\ +1 & \text{if} x > c \end{cases} \tag{13}$$

If x is not a preimage of c then define the *itinerary* of x, $I(x)$ to be the sequence $I(x) = a_0a_1a_2a_3\ldots$ where $a_i = a(f^i(x))$, $i = 0, 1, 2, 3, \ldots$. To extend this definition to pre-images of c define a metric d on $\{-1, +1\}^{\mathbb{N}_0}$ by

$$d(\mathbf{a}, \mathbf{b}) = \sum_{n=0}^{\infty} \frac{|a_n - b_n|}{2^{n+1}} \tag{14}$$

If $f^n(x) = c$ for some $x \in I$ then define the *upper itinerary*, $I(x_+)$ and the *lower itinerary*, $I(x_-)$ by

$$I(x_+) = \lim_{y \downarrow x} I(y), \quad I(x_-) = \lim_{y \uparrow x} I(y) \tag{15}$$

where the limits are taken through points which are not preimages of c. Clearly upper and lower itineraries can also be defined for points which are not preimages of c, but the $I(x_-) = I(x_+) = I(x)$.

The pair consisting of the upper and lower itinerary of the point of discontinuity itself is called the *kneading invariant* of f, $k(f)$. in other words, if $k_+(f) = I(c_+)$ and $k_-(f) = I(c_-)$ then

$$k(f) = (k_+(f), k_-(f)) \tag{16}$$

When the map f is clear from the context, the argument f will be dropped.

The order of points on the real line with different itineraries can be deduced by looking at the itineraries of the points. For this we need to define four order on sequences in $\{-1, +1\}^{\mathbb{N}_0}$, which will be relevant to the four classes of msdc maps defined earlier. Here and blow we use the notation $\mathbb{N}_0 = \{0, 1, 2, \ldots\}$ to remind the reader that indexing typically begins with the subscript zero. For sequences $\mathbf{a}$ and $\mathbf{b}$ in $\{-1, +1\}^{\mathbb{N}_0}$ and maps in class A (orientable) define $\prec_o$ by

$$\mathbf{a} \prec_o \mathbf{b} \tag{17}$$

if and only if either $a_0 < b_0$ or $a_i = b_i$, $0 \le i \le n-1$ and $a_n < b_n$. This is a complete order on $\{-1, +1\}^{\mathbb{N}_0}$ and is often called the *lexicographical order*.

For sequences $\mathbf{a}$ and $\mathbf{b}$ in $\{-1, +1\}^{\mathbb{N}_0}$ and maps in class B (semi-orientable) define $\prec_{so+}$ by

$$\mathbf{a} \prec_{so+} \mathbf{b} \tag{18}$$

if and only if either $a_0 < b_0$ or $a_i = b_i$, $0 \le i \le n-1$ and

$$a_n \Pi_0^{n-1}(-a_k) < b_n \Pi_0^{n-1}(-b_k) \tag{19}$$

so if the number of $+1$s in $a_0a_1\ldots a_{n-1}$ is odd the usual order is reversed. This is a complete order on $\{-1, +1\}^{\mathbb{N}_0}$ and is sometimes called the *unimodal order*.

For sequences **a** and **b** in $\{-1,+1\}^{\mathbb{N}_0}$ and maps in class D (semi-orientable) define $\prec_{so-}$ by

$$\mathbf{a} \prec_{so-} \mathbf{b} \tag{20}$$

if and only if either $a_0 < b_0$ or $a_i = b_i$, $0 \leq i \leq n-1$ and

$$a_n \Pi_0^{n-1}(a_k) < b_n \Pi_0^{n-1}(b_k) \tag{21}$$

so if the number of -1s in $a_1 \ldots a_{n-1}$ is odd the usual order is reversed. This is a complete order on $\{-1,+1\}^{\mathbb{N}_0}$ and is also a unimodal order.

For sequences **a** and **b** in $\{-1,+1\}^{\mathbb{N}_0}$ and maps in class D (non-orientable) define $\prec_{no}$ by

$$\mathbf{a} \prec_{no} \mathbf{b} \tag{22}$$

if and only if either $a_0 < b_0$ or $a_i = b_i$, $0 \leq i \leq n-1$ and

$$(-1)^n a_n < (-1)^n b_n \tag{23}$$

Again, this is a complete order on $\{-1,+1\}^{\mathbb{N}_0}$.

Lemma 1 *Let $f : I \to I$ be a msdc map and $\prec_\alpha$ the appropriate order. If $I(x_+) \prec_\alpha I(y_-)$ then $x < y$.*

This is a standard result and we omit the proof here. The action of the map on points induces a map on itineraries: the *shift map*, σ, defined by $\sigma(a_0 a_1 a_2 a_3 \ldots) = a_1 a_2 a_3 a_4 \ldots$. The relationship between σ and f is given by the following lemma (which is again standard).

Lemma 2 *Let $f : I \to I$ be a msdc map and $x \neq c$. Then*

$$I(f(x)_\pm) = \sigma I(x_\pm) \tag{24}$$

if f is increasing at x, and

$$I(f(x)_\pm) = \sigma I(x_\mp) \tag{25}$$

if f is decreasing at x.

This kneading theory underlies the mathematical treatment of the dynamics described below. We return to it in section 8 where this more rigorous treatment is sketched.

4. The simple cases

This section is exceptionally dull. The reader is strongly advised to look at the pictures and ignore the statements. However, the cases here are important and so cannot be omitted. In the statements of the results $\Omega(f)$ denotes the non-wandering points of f, and the proofs use standard results for monotonic maps (e.g. if non-empty, the non-wandering set of an increasing map contains only fixed points, whilst for a decreasing map there can be fixed points and possibly points of period two).

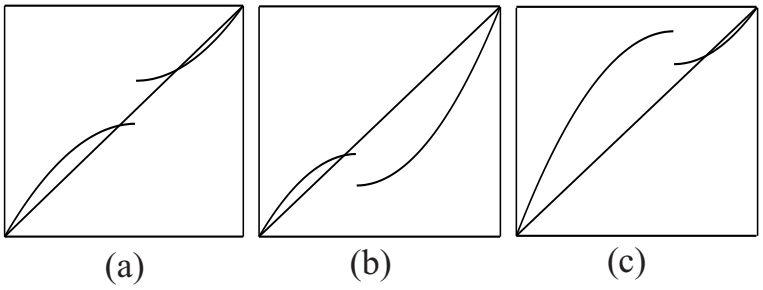

Figure 3. Quadratc maps for Lemma 3. (a) $f(c_-) < c$ and $f_(c_+) > c$; (b) $f(c_-) < c$ and $f_(c_+) < c$; and (c) $f(c_-) > c$ and $f_(c_+) > c$. Note that there is a stable fixed point in $x < c$ if $f(c_-) < c$ and a stable fixed point in $x > c$ if $f(c_+) > c$.

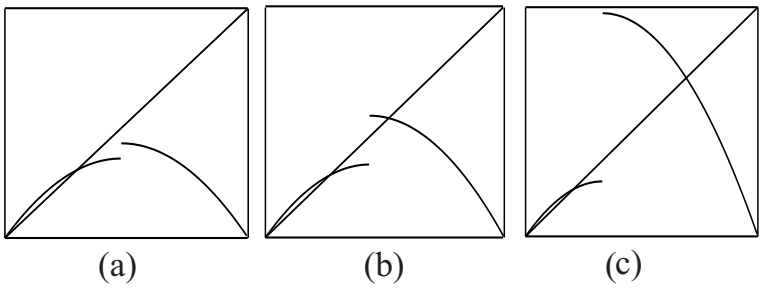

Figure 4. Quadratic maps for Lemma 4. In all three cases there is a stable fixed point in $x < c$. (a) $f(c_-) \leq c$ and $f(c_+) \leq c$; (b) $f(c_-) \leq c$, $f(c_+) > c$ and $f^2(c_+) \geq c$, there is also either a stable fixed point or a stable orbit of period two in $x > 0$; (c) $f(c_-) \leq c$, $f(c_+) > c$ and $f^2(c_+) < c$, there is no stable behaviour in $x > c$.

Lemma 3 *(The orientable case – class A) Let $f : I \to I$ be in class A and let X_+ (resp. X_-) denote the fixed points of f in $x \geq c$ (resp. $x \leq c$). If either $f(c_-) < c$ or $f(c_+) > c$ or both then $\Omega(f) = X_- \cup X_+$.*

The situation is as shown in Figure 3; proofs come from standard results for monotonic maps.

Lemma 4 *(The semi-orientable case – class B; increasing in $x < c$ and decreasing in $x > c$) Let $f : I \to I$ be in class B and let X_- denote the fixed points of f in $x \leq c$ and $X_+^{1,2}$ denote the fixed points and points of period two (possibly empty) on orbits that lie entirely in $x \geq c$.*
(a) If $f(c_-) \leq c$ and $f(c_+) \leq c$ then $\Omega(f) = X_-$.
(b) If $f(c_-) \leq c$, $f(c_+) \geq c$ then $\Omega(f) = X_- \cup X_+^{1,2}$.

Again, the different possibilities are illustrated in Figure 4, and the situation for maps in class D is the same as for class B but with the roles of $x > c$ and $x < c$ reversed. Finally we have the non-orientable case.

Lemma 5 *(The non-orientable case – class C) Let $f : I \to I$ be in class C and let X_2 denote the period two points of f in with one point on each orbit in $x \leq c$ and the other*

in $x \geq c$. Let $X_+^{1,2}$ denote the fixed points and points on orbits of period two (possibly empty) on orbits that lie entirely in $x \geq c$ and $X_-^{1,2}$ denote the fixed points and points on orbits of period two (possibly empty)on orbits that lie entirely in $x \leq c$.
(a) If $f(c_-) \geq c$ and $f(c_+) \leq c$ then $\Omega(f) = X_2$.
(b) If $f(c_-) \leq c$, $f^2(c_-) \leq c$ and $f(c_+) < c$ then $\Omega(f) = X_2 \cup X_-^{1,2}$.
(c) If $f(c_-) \leq c$, $f^2(c_-) \leq c$, $f(c_+) \geq c$ and $f^2(c_+) \geq c$ then $\Omega(f) = X_2 \cup X_-^{1,2} \cup X_+^{1,2}$.
(d) If $f(c_+) \geq c$, $f^2(c_+) \geq c$ and $f(c_-) > c$ then the situation is as in case (b) above, but with the roles of $x < c$ and $x > c$ reversed.

Having got these simple cases out of the way we can consider the possibility of more complicated sequences.

5. Sub-regions and renormalization

In this section we define sub-regions of the B-boxes and C-boxes in such a way that the boundary of chaos lies in these sub-regions and, more importantly, that the sub-regions map across each other in a well-defined way under the renormalization operations defined on each sub-region. This will enable us to define a subshift of finite type for the renormalization process in the next section. Although the various renormalizations have been defined elsewhere [10, 17], the choice of how the B-box and C-boxes should be divided into sub-regions is not unique. The choices made below ensure that the way in which the regions maps across each other by renormalization can be controlled.

From a topological point of view a map is defined via its kneading invariant as defined in section 3. To be the kneading invariant of a map in class A, B or C the kneading invariants must satsify inequalities that specify that no shift of either kneading invariant k_+ or k_- lies between k_- and k_+. Conversely, if (k_+, k_-) satisfy these inequalities then there is a map in the relevant class that has this pair of sequence as a kneading invariant (examples can be constructed from order properties of the shifts of the sequences $k_\pm$). Our basic assumption is that we can work in the space of all allowed kneading invariants, and that there is therefore a family parametrized by two sequences and hence, using a bijection from pairs of sequences to a subset of the reals, by an element of $\mathbb{R}^2$. Thus we work with families $(f_{\mathbf{a}})$ with $\mathbf{a} \in \mathcal{C} \subset \mathbb{R}^2$ such that such that for every allowed kneading invariant in the relevant class, there exists $\mathbf{a}$ such that $f_{\mathbf{a}}$ has that kneading invariant. Such a family is called a *full* family following the nomenclature for unimodal maps in [12]. Thus we will talk about A-full families $(f_{\mathbf{a}})$, meaning a family of maps in class A which is full, and the associated A-box being the set of parameters in $\mathbb{R}^2$ taken by the parameter $\mathbf{a}$, and similarly for the other classes of maps.

Let $(f_{\mathbf{a}})$ be a B-full family and without loss of generality set $c = 0$. We define five sub-regions of the B-box together with four curves on the boundary of these regions and two points on the boundary of the B-box such that the boundary of chaos is in these regions. These definitions are given in terms of the end-points, z_0 and z_1, of the interval on which the map is defined, the fixed point z^* in $x > 0$ which exists if $f_{\mathbf{a}}(0_+) > 0$, and

two points of period two: y_0 and y_1 with $y_0 < 0 < y_1$ and $f(y_i) = y_{1-i}$, $i = 0, 1$. It is relatively straightforward to show that such points exist if $f_{\mathbf{a}}(0_-) > f_{\mathbf{a}}(0_+) \geq 0$ and $f^2_{\mathbf{a}}(0_-) < 0$.

$$\begin{aligned}
B_1 &= \{\mathbf{a} \in \mathbb{R}^2 \mid f_{\mathbf{a}}(0_+) < 0\} \\
L_1 &= \{\mathbf{a} \in \mathbb{R}^2 \mid f_{\mathbf{a}}(0_+) = 0\} \\
B_2 &= \{\mathbf{a} \in \mathbb{R}^2 \mid f^2_{\mathbf{a}}(0_-) < 0,\ 0 < f_{\mathbf{a}}(0_+) < y_1\} \\
L_2 &= \{\mathbf{a} \in \mathbb{R}^2 \mid f_{\mathbf{a}}(0_+) = y_1\} \\
B_3 &= \{\mathbf{a} \in \mathbb{R}^2 \mid f^2_{\mathbf{a}}(0_-) < 0,\ f_{\mathbf{a}}(0_-) > f_{\mathbf{a}}(0_+) > y_1\} \\
L_3 &= \{\mathbf{a} \in \mathbb{R}^2 \mid f_{\mathbf{a}}(0_-) = f_{\mathbf{a}}(0_+)\} \\
B_4 &= \{\mathbf{a} \in \mathbb{R}^2 \mid f_{\mathbf{a}}(0_+) > f_{\mathbf{a}}(0_-) > z^*\} \\
L_4 &= \{\mathbf{a} \in \mathbb{R}^2 \mid f_{\mathbf{a}}(0_-) = z^*\} \\
B_5 &= \{\mathbf{a} \in \mathbb{R}^2 \mid f_{\mathbf{a}}(0_+) > z^* > f_{\mathbf{a}}(0_-)\} \\
S_1 &= \{\mathbf{a} \in \mathbb{R}^2 \mid f_{\mathbf{a}}(0_+) = z_0,\ f_{\mathbf{a}}(0_-) = 0\} \\
S_2 &= \{\mathbf{a} \in \mathbb{R}^2 \mid f_{\mathbf{a}}(0_+) > 0,\ f^2_{\mathbf{a}}(0_+) = z_0,\ f_{\mathbf{a}}(0_-) = 0\}
\end{aligned} \tag{26}$$

From [17] it follows that the boundary of chaos is contained in these regions and stretches from S_1 to S_2; parameters not covered by these regions have trivial dynamics covered by Lemma 4.

Similarly, if $(g_{\mathbf{b}})$ is a full C-family with $c = 0$ we can define seven sub-regions of the C-box and two special points, T_1 and T_2, such that the boundary of chaos in the C-box stretches from T_1 to T_2 and is contained entirely in the union of the regions. As in case B, the definitions involve two points on the interval, $y_0 < 0 < y_1$, with $g_{\mathbf{b}}(y_i) = y_i$, $i = 0, 1$. The fixed point y_0 exists if $g_{\mathbf{b}}(0_-) < 0$ and y_1 exists if $g_{\mathbf{b}}(0_+) > 0$.

$$\begin{aligned}
C_1 &= \{\mathbf{b} \in \mathbb{R}^2 \mid g_{\mathbf{b}}(0_+) < y_0,\ g_{\mathbf{b}}(0_-) < 0\} \\
M_1 &= \{\mathbf{b} \in \mathbb{R}^2 \mid g_{\mathbf{b}}(0_+) = y_0,\ g_{\mathbf{b}}(0_-) < 0\} \\
C_2 &= \{\mathbf{b} \in \mathbb{R}^2 \mid z_0 < g_{\mathbf{b}}(0_+) < 0,\ g_{\mathbf{b}}(0_-) < 0\} \\
M_2 &= \{\mathbf{b} \in \mathbb{R}^2 \mid g_{\mathbf{b}}(0_+) = 0,\ g_{\mathbf{b}}(0_-) < 0\} \\
C_3 &= \{\mathbf{b} \in \mathbb{R}^2 \mid g_{\mathbf{b}}(0_+) > 0,\ g_{\mathbf{b}}(0_-) < 0, g^2_{\mathbf{b}}(0_-) > y_1\} \\
M_3 &= \{\mathbf{b} \in \mathbb{R}^2 \mid g_{\mathbf{b}}(0_+) > 0,\ g_{\mathbf{b}}(0_-) < 0, g^2_{\mathbf{b}}(0_-) = y_1\} \\
C_4 &= \{\mathbf{b} \in \mathbb{R}^2 \mid g_{\mathbf{b}}(0_+) > 0,\ g^2_{\mathbf{b}}(0_+) > y_0,\ g_{\mathbf{b}}(0_-) < 0, g^2_{\mathbf{b}}(0_-) < y_1\} \\
T_1 &= \{\mathbf{b} \in \mathbb{R}^2 \mid g_{\mathbf{b}}(0_-) = g_{\mathbf{b}}(0_+) < 0,\ g_{\mathbf{b}}(0_-) = g^3_{\mathbf{b}}(0_-)\} \\
T_2 &= \{\mathbf{b} \in \mathbb{R}^2 \mid g_{\mathbf{b}}(0_-) = g_{\mathbf{b}}(0_+) > 0,\ g_{\mathbf{b}}(0_+) = g^3_{\mathbf{b}}(0_+)\}
\end{aligned} \tag{27}$$

Three further regions, C_5, C_6 and C_7, and three curves, M_4, M_5 and M_6 are defined by symmetry ($x \to -x$), where C_i is the symmetric image of C_{8-i}, $i = 5, 6, 7$, and M_j is the symmetric image of M_{7-j}, $j = 4, 5, 6$.

Similar regions, lines and points are defined for maps in class D, corresponding to the sets defined for class B after the transformation $x \to -x$. We shall not list these regions, curves and points here, they will be denoted by the symbols D_k, $k = 1, \ldots, 5$, N_r, $r = 1, \ldots, 4$, and R_s, $s = 1, 2$, respectively in the obvious way.

The next step is to define induced maps for maps in each region, determine the range of behaviour that these induced maps can exhibit and associate to each renormalization operation a pair of functions which define the iterates of the induced map in terms of

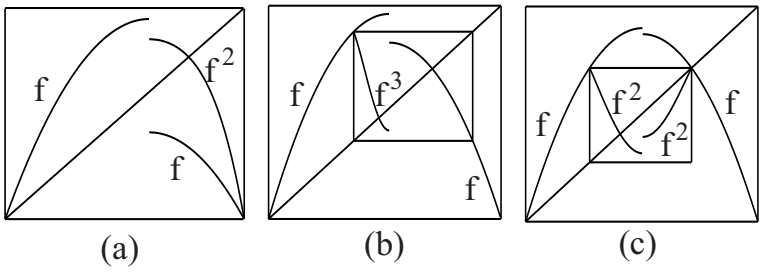

Figure 5. Renormalized maps for B_1, B_2 and B_3.

the iterates of the original map and the periodic orbits which are left behind by the renormalization.

Suppose that $\mathbf{a} \in B_1$, then $f_{\mathbf{a}}((0, z_1]) \subseteq [z_0, 0)$ and so $f_{\mathbf{a}}^2$ restricted to $(0, z_1]$ is monotonic and decreasing (as $f_{\mathbf{a}}$ is decreasing in $x > 0$ and increasing in $x < 0$, so the the induced map $R_{B_1} f_{\mathbf{a}} : I \to I$ defined by

$$R_{B_1} f_{\mathbf{a}}(x) = \begin{cases} f_{\mathbf{a}}(x) & \text{if } x < 0 \\ f_{\mathbf{a}}^2(x) & \text{if } x > 0 \end{cases} \tag{28}$$

is a map in class B. Moreover, $f_{\mathbf{a}}^2(0_+) \leq f_{\mathbf{a}}(0_-)$, with equality if $f_{\mathbf{a}}(0_+) = 0$, and in the limit of $f_{\mathbf{a}}(0_+) = z_0$ (i.e. $z_1 \to 0$), $f_{\mathbf{a}}^2(0_+) = z_0$. Hence $R_{B_1} f_{\mathbf{a}}$ is in either B_1, B_2, B_3, L_1 or L_2 (see Figure 5). Furthermore, maps on the boundary of chaos in B_1 are mapped by R_{B_1} across the boundary of chaos in $B_1 \cup L_1 \cup B_2 \cup L_2 \cup B_3$. In general, if the map $f_{\mathbf{a}}$ is itself an induced map defined by the n_1^{th} iterate of a map in $x > 0$ and the n_2^{th} iterate of a map in $x < 0$, then the induced map $R_{B_1} f_{\mathbf{a}}$ has iterates $\beta_1(n_1, n_2)$ where $\beta_1 : \mathbb{N}^2 \to \mathbb{N}^2$ is defined by

$$\beta_1(n_1, n_2) = (n_1 + n_2, n_2) \tag{29}$$

Since the induced map is defined on the whole interval for which $f_{\mathbf{a}}$ is defined we do not lose any periodic orbits so we do not define any operator to give the period of periodic orbits left behind in this case. The important information is thus that the boundary of chaos in B_1 is mapped under renormalization to the boundary of chaos in $B_1 \cup L_1 \cup B_2 \cup L_2 \cup B_3$ and the value of β_1, which gives the iterates of the induced map.

Now consider $\mathbf{a} \in B_2$. This case is typical of the arguments required in the other cases so we go through it in more detail.By the remarks already made (above the definitions of the regions B_i) there is an orbit of period two $\{y_0, y_1\}$ with $y_0 < 0 < y_1$. Define the map $R_{B_2} f_{\mathbf{a}} : [y_0, y_1] \to I$ by

$$R_{B_2} f_{\mathbf{a}}(x) = g(x) = \begin{cases} f_{\mathbf{a}}^3(x) & \text{if } x \in [y_0, 0) \\ f_{\mathbf{a}}(x) & \text{if } x \in (0, y_1] \end{cases} \tag{30}$$

(see Figure 5). Clearly g is continuous and decreasing in $(0, y_1]$, and since $f_{\mathbf{a}}$ is continuous and increasing in $x < 0$, $f_{\mathbf{a}}([y_0, 0)) = [y_1.f(0_-))$ lies in $x > 0$ where $f_{\mathbf{a}}$ is continuous and decreasing, so $f_{\mathbf{a}}^2([y_0, 0)) = (f_{\mathbf{a}}^2(0_-), y_0]$ lies in $x < 0$ fo the left of y_0 and so $f_{\mathbf{a}}^3$ is

continuous and decreasing restricted to $[y_0, 0)$ and so g is continuous and decreasing on this interval and $g([y_0, 0)) = (f_{\mathbf{a}}^3(0_-), y_1]$.

Thus g maps $[y_0, y_1]$ into itself provided $f_{\mathbf{a}}^3(0_-) \geq y_0$ and $f_{\mathbf{a}}(0_+) \leq y_1$. The second of these conditions is guaranteed by the definition of B_2 whilst if $f_{\mathbf{a}}^3(0_-) < y_0$ then $[y_0, y_1] \subseteq g([y_0, 0)$ and since $f_{\mathbf{a}}(0_+) > 0$ and $f_{\mathbf{a}}(y_1) = y_0 < 0$ there exists $v \in (0, y_1)$ such that $f_{\mathbf{a}}(v) = 0$ and $[y_0, c] \subseteq g([v, y_1])$. The two stated inclusions are enough to prove that g has positive topological entropy using standard Markov partition techniques and hence when considering the boundary of chaos we may assume that g maps $[y_0, y_1]$ into itself and is in class C as both branches are decreasing.

Since $g(0_+) > 0$ and $f_{\mathbf{a}}$ is a full family, varying $\mathbf{a}$ in B_2 allows g to be any map on the boundary of chaos in C with $g_{\mathbf{b}}(0_+) > 0$. Hence the boundary of chaos in B_2 is mapped under renormalization to the part of the boundary of chaos in class C contained in $C_3 \cup M_3 \cup C_4 \cup M_4 \cup C_5 \cup M_5 \cup C_6 \cup M_6 \cup C_7$.

The effect of this renormalization on iterates of a general induced map is given by

$$\beta_2(n_1, n_2) = (n_1, n_1 + 2n_2) \tag{31}$$

The only recurrent dynamics which is not contained in the union of forward iterates of (y_0, y_1) consists of fixed points (z_0) which we knew about already (from the definition of maps in class B) and so the new information is that there is an orbit of period two. More generally, an orbit of period $n_1 + n_2$ is 'left behind' by this renormalization step. Hence we define $p_{B_2} : \mathbb{N}^2 \to \mathbb{N}$ by

$$p_{B_2}(n_1, n_2) = n_1 + n_2 \tag{32}$$

Rather than work painfully through the remaining cases, the idea should be clear enough by now and the results are described in Table 1 (the renormalization in region B_3 is sketched in Figure 5). Note that the only subtle aspect of this paper is the second column of this table. The sub-regions of the boxes must be defined in such a way that the boundary of chaos in one region is mapped onto the boundary of chaos in a union of other sub-regions with no remainder. As mentioned earlier this is not a unique representation, but captures the dynamics with a minimum of fuss.

6. A subshift of finite type under renormalization

The first two columns of Table 1 define a subshift of finite type for the renormalization of these single discontinuity maps: given (almost) any sequence of symbols allowed by these columns there is a map on the boundary of chaos which can be renormalized with this sequence of operations. Maps which renormalize to class A may be further renormalizable, but since these transitions are well understood [13, 27] we will ignore them here. Now, for maps which do not fall into class A under renormalization there are two possibilities: either they can be renormalized a finite number of times and then fall on the special points S_k, T_k or R_k $(k = 1, 2)$, defined in the previous section, or they can be renormalized an infinite number of times without falling on these points. For maps on the boundary of chaos in the former case there is a finite set of periods, and the transition

Table 1. Effect of renormalization in the different regions described in the text. The image is the set of regions mapped onto by renormalization, the renormalization itself gives the induced map as iterates on the right and left respectively as a function of the original right and left iterates, and the period indicates the period of periodic orbits 'left behind' by renormalization.

Region	**Image**	**Renormalization**	**Period**
B_1	$B_1 \cup L_1 \cup B_2 \cup L_2 \cup B_3$	$\beta_1(n_1, n_2) = (n_1 + n_2, n_2)$	$\emptyset$
L_1	M_2	$\lambda_1(n_1, n_2) = (n_1, n_1 + 2n_2)$	$n_1 + n_2$
B_2	$C_3 \cup C_4 \cup C_5 \cup C_6 \cup C_7$ $\cup M_3 \cup M_4 \cup M_5 \cup M_6$	$\beta_2(n_1, n_2) = (n_1, n_1 + 2n_2)$	$n_1 + n_2$
L_2	N_4	$\lambda_2(n_1, n_2) = (2n_1, n_1 + n_2)$	n_1
B_3	D_4	$\beta_3(n_1, n_2) = (2n_1, n_1 + n_2)$	n_1
L_3	N_3	$\lambda_3(n_1, n_2) = (2n_1, n_1 + n_2)$	n_1
B_4	$D_1 \cup N_1 \cup D_2 \cup N_3 \cup D_3$	$\beta_4(n_1, n_2) = (2n_1, n_1 + n_2)$	n_1
L_4	R_3	$\lambda_4(n_1, n_2) = (2n_1, n_1 + n_2)$	n_1
B_5	A	$\beta_5(n_1, n_2) = (2n_1, n_2)$	n_1
C_1	A	$\gamma_1(n_1, n_2) = (n_1 + n_2, 2n_2)$	n_2
M_1	S_1	$\mu_1(n_1, n_2) = (n_1, 2n_2)$	n_2
C_2	B_1	$\gamma_1(n_1, n_2) = (n_1, 2n_2)$	n_2
M_2	L_1	$\mu_2(n_1, n_2) = (n_1, 2n_2)$	n_2
C_3	$B_2 \cup L_2 \cup B_3 \cup L_3 \cup B_4$	$\gamma_3(n_1, n_2) = (n_1, 2n_2)$	n_2
M_3	S_2	$\mu_3(n_1, n_2) = (n_1, 2n_2)$	n_2
C_4	A	$\gamma_4(n_1, n_2) = (2n_1, 2n_2)$	$\{n_1, n_2\}$
M_4	R_2	$\mu_4(n_1, n_2) = (2n_1, n_2)$	n_1
C_5	$D_2 \cup N_2 \cup D_3 \cup N_3 \cup D_4$	$\gamma_4(n_1, n_2) = (2n_1, n_2)$	n_1
M_5	N_1	$\mu_5(n_1, n_2) = (2n_1, n_2)$	n_1
C_6	D_1	$\gamma_6(n_1, n_2) = (2n_1, n_2)$	n_1
M_6	R_1	$\mu_6(n_1, n_2) = (2n_1, n_2)$	n_1
C_7	A	$\gamma_7(n_1, n_2) = (2n_1, n_1 + n_2)$	n_1
D_1	$D_1 \cup N_1 \cup D_2 \cup N_2 \cup D_3$	$\delta_1(n_1, n_2) = (n_1, n_1 + n_2)$	$\emptyset$
N_1	M_5	$\nu_1(n_1, n_2) = (2n_1 + n_2, n_2)$	$n_1 + n_2$
D_2	$C_1 \cup C_2 \cup C_3 \cup C_4 \cup C_5$ $\cup M_1 \cup M_2 \cup M_3 \cup M_4$	$de_2(n_1, n_2) = (2n_1 + n_2, n_2)$	$n_1 + n_2$
N_2	L_3	$\nu_2(n_1, n_2) = (n_1 + n_2, 2n_2)$	n_2
D_3	B_4	$\delta_3(n_1, n_2) = (n_1 + n_2, 2n_2)$	n_2
N_3	L_3	$\nu_3(n_1, n_2) = (n_1 + n_2, 2n_2)$	n_2
D_4	$B_1 \cup L_1 \cup B_2 \cup L_3 \cup B_3$	$\delta_4(n_1, n_2) = (n_1 + n_2, 2n_2)$	n_2
N_4	S_1	$\nu_4(n_1, n_2) = (n_1 + n_2, 2n_2)$	n_2
D_5	A	$\delta_5(n_1, n_2) = (n_1, 2n_2)$	n_2

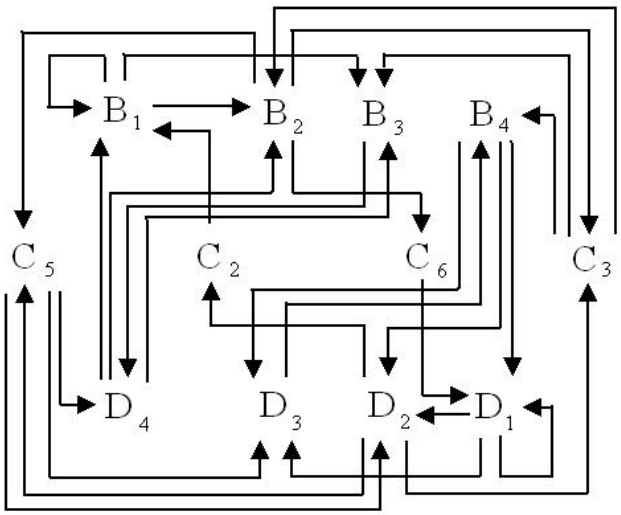

Figure 6. Directed graph for the subshift defined by renormalization of monotonic maps with a single discontinuity.

from zero entropy to positive entropy involves a discontinuous jump in the number of periods present in the maps. In the latter case the maps can be renormalized an infinite number of times, leaving behind an infinite set of periodic orbits. It is this case that we pursue further here. Thus, in what follows, we ignore the boundary elements L_i, M_k and N_i, and concentrate on maps which are infinitely renormalizable and which never renormalize to these boundaries. These ignored cases are easy to reintroduce into the analysis using Table 1.

Since class A is also to be ignored, we can ignore B_5, C_1, C_4, C_7 and D_5 on the grounds that any map which falls into one of these classes under renormalization then renormalizes to class A. The graph associated with the remaining regions is shown in Figure 6: the arrows indicating the allowed paths. Note that the diagram is symmetric under the transformation.

$$(B_i, C_2, C_3, C_5, C_6, D_i) \to (D_i, C_6, C_5, C_3, C_2, B_i) \tag{33}$$

Once again, this simply reflects the relationships between the maps under the transformation $x \to -x$.

We now have to be a little careful: since the renormalization map is discontinuous, there may be the (inevitable) ambiguity about whether a sequence allowed by the subshift actually corresponds to a map inside the region, or whether it reflects the behaviour on the boundary of the region. The two fixed points of this subgraph B_1^∞ and D_1^∞, are a case in point, since they represent the points R_1 and S_1 respectively. Indeed any sequence allowed by this diagram which ends with an infinite sequence of B_1s or D_1s corresponds to the case mentioned above for which there is a finite set of periods

for maps on the boundary of chaos. There are two pairs of periodic orbits of period two allowed by the subgraph of Figure 6: $(D_3B_4)^\infty$ and its symmetric image $(B_3D_4)^\infty$ correspond to period-doubling. In the context of the discontinuous maps defined here this sequence of bifurcations is unstable to perturbations of the maps although in the context of continuous maps of the intervals (for class B or D) or symmetric maps in class C this route is stable to perturbations. Thus we identify these sequences with the boundary orbit $(L_3N_3)^\infty$. Looking at the remainder of possible boundary behaviour we see that any other sequence (i.e. one which does not contain the four infinite sequences described above) does indeed correspond to an orbit of the subshift which is not on the boundary at any stage of renormalization.

Thus sequences which contain the subsequences B_1^∞, D_1^∞, $(D_3B_4)^\infty$ and $(B_3D_4)^\infty$ are not allowed. (Alternatively we could have worked with closed regions, in which case a subshift is obtained for which all sequences are allowed but some must be identified.)

The second pair of periodic cycles of period two is $(C_3B_2)^\infty$ and $(C_5D_2)^\infty$. These correspond to maps which undergo the anharmonic route to chaos described in [15, 16] and is robust to small perturbations of the defining families. So any sequence allowed by Figure 6 which ends with either of these sequences defines a line segment in parameter space on which maps undergo the anharmonic route to chaos after some initial 'out of sequence' set of bifurcations. We believe that these are the only line segments on the boundary of chaos which do not lie in A-boxes.

Figure 6 together with Table 1 gives a complete catalogue of the periods and renormalizations of maps on the boundary of chaos for the families of maps we are considering with one exception (described in section six). In the remainder of this paper we consider two sets of possibilities in more detail: the low-period cycles of Figure 6 and the anomalous anharmonic routes to chaos.

7. Low-period orbits of the subshift

When describing low order periodic orbits of the subshift we shall adopt the convention that sequences are read from left to right (as though they were maps acting on the left), so $(B_3D_4B_1)^\infty$ is an allowed sequence whilst $(B_1D_4B_3)^\infty$ is not. Since the subshift is symmetric, periodic sequences either come in pairs or they are themselves symmetric. We shall consider the periodic sequences of length two and three together with the symmetric cycle of length four and six.

7.1. Cycles of period two and symmetric cycles of period four

There are two independent cycles of period two allowed by the graph in Figure 6: the cycles $(C_3B_2)^\infty$ and $(C_5D_2)^\infty$. Maps on the boundary of chaos in these cases have been described elsewhere [15, 16] and will be considered in the next section. There is one symmetric cycle of period four: $(C_3B_2C_5D_2)^\infty$, and it is this case that we concentrate on here.

Suppose that some map $g \in C_3$ is infinitely renormalizable with a sequence of renormalizations corresponding to this renormalization cycle. Then there is a natural period in the renormalization process: after four renormalizations we come back and repeat the same renormalizations. So, suppose that after 4k renormalization steps we have a renormalized map in C_3 involving the iterates (n_1, n_2). Applying γ_3 we obtain a new map in B_2 with iterates $(n_1, 2n_2)$ and leave behind an orbit of period n_2. Now applying β_2 we get a new map in C_5 with iterates $(n_1, n_1 + 4n_2)$ and an orbit of period $n_1 + 2n_2$. Applying γ_5 gives a map in D_2 with iterates $(2n_1, n_1 + 4n_2)$ and an orbit of period n_1. Finally, applying δ_2 we get a map with iterates $(5n_1+4n_2, n_1+4n_2)$, an orbit of period $3n_1+4n_2$ and we are back where we started. Hence, through one renormalization cycle the iterates of the induced map changes from $(n_1, 2n_2)$ to $(5n_1 + 4n_2, n_1 + 4n_2)$ and periodic orbits of period n_2, n_1, $n_1 + 2n_2$ and $3n_1 + 4n_2$ have been left behind. This can be represented conveniently in the following way: after $4k$ renormalization steps the iterates of the induced map are (n_1^k, n_2^k) where

$$\begin{pmatrix} n_1^{k+1} \\ n_2^{k+1} \end{pmatrix} = A \begin{pmatrix} n_1^k \\ n_2^k \end{pmatrix} \tag{34}$$

with

$$A = \begin{pmatrix} 5 & 4 \\ 1 & 4 \end{pmatrix} \tag{35}$$

and the periodic orbits created in the four renormalizations between the $4k^{th}$ and $4(k+1)^{th}$ are $p_{4k+1}, \ldots, p_{4k+4}$ where

$$\begin{pmatrix} p_{4k+1} \\ p_{4k+2} \\ p_{4k+3} \\ p_{4k+4} \end{pmatrix} = B \begin{pmatrix} n_1^k \\ n_2^k \end{pmatrix}, \quad B = \begin{pmatrix} 0 & 1 \\ 1 & 0 \\ 1 & 2 \\ 3 & 4 \end{pmatrix} \tag{36}$$

and $n_1^0 = n_2^0 = 1$. Applying these operations we find that this gives a map on the boundary of chaos with periodic orbits with periods

$$1, 1, 3, 7, 5, 9, 19, 47, 29, 65, 123, 311, \ldots \tag{37}$$

Another route to chaos associated with this renormalization cycle can be found in class B_2, infinitely renormalizable with $(B_2C_5D_2C_3)^\infty$. In this case

$$A = \begin{pmatrix} 5 & 2 \\ 2 & 4 \end{pmatrix}, \quad B = \begin{pmatrix} 1 & 0 \\ 1 & 1 \\ 1 & 2 \\ 3 & 2 \end{pmatrix} \tag{38}$$

giving the sequence of periods

$$1, 2, 3, 5, 7, 13, 19, 33, 47, 85, 123, 217, \ldots \tag{39}$$

The remaining two permutations of the renormalization cycle give the symmetric images of these two routes and hence the same sequence of periods.

7.2. Cycles of period three and symmetric cycles of period six

There are two independent cycles of period three, $(B_1B_3D_4)^\infty$ and $(B_4D_2C_3)^\infty$ together with their symmetric images, which we shall ignore. There are also two symmetric cycles of period six, $(C_5D_4B_2C_3B_4D_2)^\infty$ and $(B_2C_6D_1D_2C_2B_1)^\infty$. The three routes to chaos associated with $(B_1B_3D_4)^\infty$ will be described in the same way as we approached the previous example. Since no periodic orbit is associated with a renormalization in B_1 each run through the cycle will produce two periodic orbits. After each run through the cycle the iterate of the induced map will be changed, so the matrix A is defined as before (except it describes the change after three rather than four renormalization steps) whilst the matrix B in now 2×2 and

$$\begin{pmatrix} p_{2k+1} \\ p_{2k+2} \end{pmatrix} = BA^k \begin{pmatrix} 1 \\ 1 \end{pmatrix} \tag{40}$$

For $(B_1B_3D_4)^\infty$ (and hence maps in B_1) we find

$$A = \begin{pmatrix} 3 & 4 \\ 2 & 4 \end{pmatrix}, \quad B = \begin{pmatrix} 1 & 1 \\ 1 & 2 \end{pmatrix} \tag{41}$$

giving the sequence

$$2, 3, 13, 19, 83, 121, 529, 771, \ldots \tag{42}$$

For maps in B_3 which are infinitely renormalizable with $(B_3D_4B_1)^\infty$ we find

$$A = \begin{pmatrix} 5 & 3 \\ 2 & 2 \end{pmatrix}, \quad B = \begin{pmatrix} 1 & 0 \\ 1 & 1 \end{pmatrix} \tag{43}$$

giving the sequence

$$1, 2, 8, 12, 52, 76, 332, 484, \ldots \tag{44}$$

and for maps in D_4 which are infinitely renormalizable with $(D_4B_1B_3)^\infty$

$$A = \begin{pmatrix} 2 & 6 \\ 1 & 5 \end{pmatrix}, \quad B = \begin{pmatrix} 0 & 1 \\ 1 & 3 \end{pmatrix} \tag{45}$$

giving the sequence

$$1, 4, 6, 24, 38, 166, 242, 1068, \ldots \tag{46}$$

Maps which are infinitely renormalizable with $(B_4D_2C_3)^\infty$ and its permutations are described in precisely the same way, but now B is a 2×3 matrix and the periodic orbits are in the sequence

$$\begin{pmatrix} p_{3k+1} \\ p_{3k+2} \\ p_{3k+3} \end{pmatrix} = BA^k \begin{pmatrix} 1 \\ 1 \end{pmatrix} \tag{47}$$

For maps in B_4 which are infinitely renormalizable with $(B_4D_2C_3)^\infty$

$$A = \begin{pmatrix} 5 & 1 \\ 2 & 2 \end{pmatrix}, \quad B = \begin{pmatrix} 1 & 0 \\ 1 & 1 \\ 3 & 1 \end{pmatrix} \tag{48}$$

giving periods

$$1, 2, 4, 5, 10, 22, 34, 54, 122, 190, 298, 678, \ldots \tag{49}$$

For the corresponding maps in D_2

$$A = \begin{pmatrix} 4 & 2 \\ 2 & 3 \end{pmatrix}, \quad B = \begin{pmatrix} 0 & 1 \\ 1 & 1 \\ 2 & 1 \end{pmatrix} \tag{50}$$

giving the sequence of periods

$$1, 2, 3, 5, 11, 17, 27, 61, 95, 149, 339, 529, \ldots \tag{51}$$

And for maps in C_2 we find

$$A = \begin{pmatrix} 5 & 2 \\ 1 & 2 \end{pmatrix}, \quad B = \begin{pmatrix} 0 & 1 \\ 1 & 0 \\ 3 & 2 \end{pmatrix} \tag{52}$$

giving

$$1, 1, 5, 3, 7, 27, 13, 41, 149, 67, 231, 827, \ldots \tag{53}$$

The way to relate the subshift to the periodic orbits on the boundary of chaos should now be clear and we will not go through the full calculation for the two remaining cases, $(C_5D_4B_2C_3B_4D_2)^\infty$ and $(B_2C_6D_1D_2C_2B_1)^\infty$. However, just to emphasize the point that the sequences of periods are sometimes quite curious we end this section with the first few terms from the latter case:

$$1, 3, 5, 21, 13, 51, 77, 357, 205, 819, 1229, 5733, \ldots \tag{54}$$

7.3. The anharmonic route to chaos: generalisations

The anharmonic route to chaos, described in [15, 16], is stable to perturbations and so we expect any sequence allowed by the subshift which ends $(B_2C_3)^\infty$ or $(D_2C_5)^\infty$ to correspond to segments of curves on the boundary of chaos in parameter space. Consider the case of $(B_2C_3)^\infty$, for example. In the notation of the previous section we find that

$$A = \begin{pmatrix} 1 & 0 \\ 2 & 4 \end{pmatrix}, \quad B = \begin{pmatrix} 1 & 1 \\ 1 & 2 \end{pmatrix} \tag{55}$$

and so we obtain the sequence of periods

$$2, 3, 7, 13, 27, 53, \ldots \tag{56}$$

or

$$p_{n+1} = 2p_n + (-1)^n, \quad p_1 = 2 \tag{57}$$

Note the n_1 is not charged by this renormalization process, but that $f(0_+) > 0$ since $f \in B_2$. Hence there is a fixed point (and possibly a point of period two) of f in $x > 0$ which is not picked out by the renormalization scheme. This is the one exception to

the set of periods obtained from Figure 6 and Table 1 which must be introduced by hand. More generally, if there is some finite number of renormalization steps followed by $(B_2C_3)^\infty$ an orbit of period n_1 and, possibly, an orbit of period $2n_1$, exist for the corresponding map on the boundary of chaos which will not appear in the list generated by the algorithm of section four.

As an example consider the allowed sequence $C_2B_1(B_2C_3)^\infty$. Applying the renormalization rules we find that there are periodic orbits of period one and (p_n), with

$$p_{n+1} = 2p_n + 3(-1)^n, \quad p_1 = 5 \tag{58}$$

and that $n_1 = 3$ during the cycle $(B_2C_3)^\infty$. Hence the maps corresponding to this sequence also have an orbit of period three and, possibly, an orbit of period six. All preimages of $(B_2C_3)^\infty$ allowed by the subshift can be treated similarly.

8. Towards rigorous statements

The analysis of the past few sections is based on the intuitive description of renormalization given in section 5. To show that for every sequence allowed by the subshift for renormalization there exists a map which can be renormalized with that sequence of renormalizations we need to establish that the process of renormalization always leads to kneading sequences that satisfy the properties required in section 6. So in principle this could be made rigorous by looking at the possible renormalizations of kneading invariants on the symbolic level and demonstrating that the new kneading invariants constructed (including their limits) are still kneading invariants of msdc maps.

To illustrate the ideas involved, consider the renormalization of maps in B_1 with discontinuity at 0: since $f(0_+) < 0$ in B_1 and f is decreasing in $x > 0$ the kneading invariants for maps which are not boring in the sense of Lemma 4 are of the form

$$\begin{aligned} k_+ &= (+1-1)(-1)^{n_1}(+1-1)^{n_2}(-1)^{n_3}\dots \\ k_- &= (-1)(+1-1)^{m_1}(-1)^{m_2}(+1-1)^{m_3}\dots \end{aligned} \tag{59}$$

(with the convention that if one of the n_i or m_j is infinite then there are no further symbols) satisfying the relevant inequalities of section 6. The induced map $R_{B_1}f : I \to I$ defined by

$$R_{B_1}f(x) = \begin{cases} f(x) & \text{if } x < 0 \\ f^2(x) & \text{if } x > 0 \end{cases} \tag{60}$$

is a map in class B with $f^2(0_+) \le f_{\mathbf{a}}(0_-)$, with equality if $f_{\mathbf{a}}(0_+) = 0$, and in the limit of $f_{\mathbf{a}}(0_+) = z_0$ (i.e. $z_1 \to 0$), $f^2_{\mathbf{a}}(0_+) = z_0$. Hence $R_{B_1}f_{\mathbf{a}}$ is in either B_1, B_2, B_3, L_1 or L_2 and, by definition, has kneading invariant (K_+, K_-) given by

$$\begin{aligned} K_+ &= (+1)(-1)^{n_1}(+1)^{n_2}(-1)^{n_3}\dots \\ K_- &= (-1)(+1)^{m_1}(-1)^{m_2}(+1)^{m_3}\dots \end{aligned} \tag{61}$$

Thus we would need to establish that for every map on the boundary of chaos in B_1 with kneading invariant (59) there is a map on the boundary of chaos in $B_1 \cup B_2 \cup B_3 \cup L_1 \cup L_2$ with kneading invariant (61).

The second part of the argument would be to establish the converse: that for every map on the boundary of chaos in $B_1 \cup B_2 \cup B_3 \cup L_1 \cup L_2$ with kneading invariant given by (61) satisfying the appropriate inequalities for this subset of class B then there is a map in B_1 with kneading invariant (59).

These two steps, which can be expressed formally in terms of inequalities on the two kneading invariants (59) and (61) then need to be repeated for every one of the different renormalizations of Table 1. This, together with a compactness argument to ensure limiting sequences make sense, would then rigorously establish the esistence of maps on the boundary of chaos described via the subshift of finite type of Figure 6. However, the many different renormalizations, coupled with the proliferation of subcases, makes this project unfeasibly long. It may be that there is a better global approach that could avoid this proliferation, but we have not found one, and so leave this as an open problem, whilst conjecturing that it is true!

9. Conclusion and caveats

In this paper a subshift of finite type for the(zero entropy) renormalization of two classes of single discontinuity maps related to differential equations has been given explicitly. This makes it possible to give a complete description of the periods present for maps on the boundary of chaos in these classes. Whilst this seems new and interesting a number of caveats are worth making (the reader may prefer to see these as assumptions).

1. The mathematics described works entirely on the symbolic level of kneading theory. We are not aware of any results which prove that full families (i.e. families that exhibit all topologically possible behaviours) of such maps exist, nor that the natural parametrization of such maps if they do exist can be mapped to the plane. In particular, it has not been proved that the quadratic examples of section two satisfy all the assumptions needed. In consequence, it may turn out that not all the (uncountably many) routes to chaos described by the subshift are realizable for differentiable maps in the relevant classes.

2. When talking about points and lines on the boundary of chaos we have been assuming metric properties of the subshift without justification. From [27] we know that there are lines in each A-box on which the transition to chaos is abrupt, via a mechanism related to circle intermittency. Similarly we know that in each B-box and C-box there are segments of lines on which the transition to chaos is via the anharmonic bifurcation [16]. On the other hand, it is not known whether there are any other robust routes to chaos: numerical evidence suggests that these are the only two. Hence we have assumed that all other routes correspond to point on the boundary of chaos.

3. Section 5 gives an algorithm for calculating the periods of periodic orbits for maps on the boundary of chaos. The representation does not always give monotonic sequences and there may well be a better way of describing the periods.

4. (Historical note) This paper is adapted from a preprint which formed a chapter of my Adams Prize Essay in 1992. It was not submitted for publication at the time because I could not prove that any given family is full (indeed, there are results to prove that standard families are not full [10, 11, 14]). However, the renewed interest in piecewise monotonic maps in hybrid systems, and the remark in point 1 above, which shows that every admissible sequence in the kneading invariant of a piecewise continuous map, means that the results are relevant to broader classes of msdc maps.

Acknowledgements This research was partially funded by the CICADA project, EPSRC grant EP/E050441/1.

[1] V.S. Afraimovich, V.V. Bykov and L.P. Shilnikov (1982) 'On structurally unstable attracting limit set of the type of Lorenz attractor', Trans. Moscow. Math. Soc. **44** 153-216.

[2] V.S. Afraimovich and L.P. Shilnikov (1983). 'Strange attractors and quasi-attractors' in *Nonlinear Dynamics and Turbulence*, eds. G.I. Barenblatt, G. Iooss and D.D. Joseph, London, Pitman.

[3] V. Avrutin and M. Schanz (2006) 'On multi-parametric bifurcations in a scalar piecewise-linear map', Nonlinearity **19** 531-552.

[4] V. Avrutin and M. Schanz (2008) 'On the fully developed bandcount adding scenario', Nonlinearity **21** 1077-1103.

[5] V. Avrutin, M. Schanz and S. Bannerjee (2006) 'Multi-parametric bifurcations in a piecewise-linear discontinuous map', Nonlinearity **19** 1875-1906.

[6] S. Bannerjee, M.S. Karthik, G. Yuan and J.A. Yorke (2000) 'Bifurcations in one-dimensional piecewise smooth maps – theory and applications in switching circuits',

[7] M. di Bernardo, C.J. Budd and A.R. Champneys (1998) 'Grazing, skipping and sliding: analysis of the nonsmooth dynamics of the dc/dc buck converter', Nonlinearity **11** 858-890.

[8] M. di Bernardo, C.J. Budd and A.R. Champneys (2001) 'Normal form maps for grazing bifurcations in n-dimensional piecewise-smooth dynamical systems', Physica D **160** 222-254.

[9] M. di Bernardo, C.J. Budd, A.R. Champneys, P. Kowalczyk (2008) *Piecewise-smooth Dynamical Systems: Theory and Applications*, Springer, London.

[10] D. Berry (1990) 'Nonwandering sets of Lorenz maps' Ph.D. thesis, University of Warwick.

[11] D. Berry and B.D Mestel (1991) 'Wandering Intervals for Lorenz maps with Bounded Nonlinerity', Bull. LMS **23** 183-189.

[12] P. Collet and J.-P. Eckmann (1981) *Iterated maps on the interval as dynamical systems*, Birkhäuser, Basel.

[13] J.M. Gambaudo, I. Procaccia, S. Thomae and C. Tresser (1987) 'New universal scenarios for the onset of chaos in Lorenz-type flows' Phys. Rev. Lett. **57** 925-928.

[14] P. Glendinning (1992) *Chaos and Routes to Chaos in Lorenz maps*, Adams Prize Essay, University of Cambridge.

[15] P. Glendinning (1992) 'Robust new routes to chaos in differential equations', Phys. Lett. A **168** 40-46.

[16] P. Glendinning (1993) 'The anharmonic route to chaos: kneading theory', Nonlinearity **6** 349-367.

[17] P. Glendinning, J.E. Los and C. Tresser (1990) 'Renormalization between classes of maps' Phys. Lett. A **145** 109-122.

[18] P. Glendinning and N. Sidorov (2013) 'The doubling map with asymmetrical holes', Ergod. Th. & Dyn. Syst., 1-21, doi:10.1017/etds.2013.98.

[19] P. Glendinning and C. Sparrow (1993) 'Prime and renormalisable kneading invariants and the dynamics of expanding Lorenz maps', Physica D **62** 22-50.

[20] J. Guckenheimer and R.F. Williams (1979) 'Structural stability of Lorenz attractors', Pub. Math. IHES **50**, 59-72.

[21] J.H. Hubbard and C.T. Sparrow (1990) 'The Classification of Topologically Expansive Lorenz Maps', Comm. Pure Appl. Math., **XLIII** 431-443.

[22] J.L. Kaplan and J.A. Yorke (1979) 'Preturbulence: a regime observed in a fluid flow model of Lorenz', Comm. Math. Phys. **67** 93-108.

[23] E.N. Lorenz (1963) 'Deterministic nonperiodic flow', J. Atmos. Sci. **20** 130-141.

[24] D.V. Lyubimov, A.S. Pikovsky and M.A. Zaks (1989) 'Universal scenarios of transition to chaos via homoclinic bifurcations', Sov. Sci. Rev. C. Math. Phys. **8** 221-292.

[25] J. Milnor and W. Thurston (1988) 'On iterated maps of the interval', in *Dynamical Systems*, ed. J.C. Alexander, Springer LNM 1342, Berlin.

[26] C. Sparrow (1982) *The Lorenz equations: bifurcations, chaos, and strange attractors*, Applied Math. Sci. **41**. New York: Springer-Verlag.

[27] C. Tresser (1983) 'Nouveaux types de transitions vers une entropie topologique positive' C.R.Acad. Sci. (Paris) Série I, **296**, 729-732.

[28] R.F. Williams (1979) 'The structure of Lorenz attractors', Pub. Math. IHES **50**, 73-99.